

UNIVERSITY OF TWENTE

THE APPLICATION OF AN ACCELEROMETER
USED AS NAVIGATION

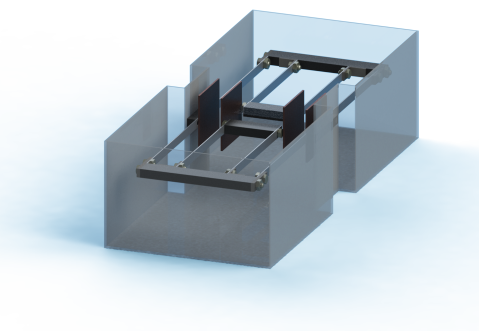
Accelerometer for Navigation

Author:

Simo GABRIEL
Laduona DAI
Samuel OYEDIRAN
Niels WILLEMEN
Jasper RINGOOT
Jasper JONKER

Supervisor:

Dr. ir. Remco WIEGERINK
Kevin HOFHUIS



July 2, 2015

Contents

| | | |
|-----------|--|-----------|
| 1 | Introduction | 4 |
| 2 | Theory | 5 |
| 2.1 | Specifications | 5 |
| 2.2 | Mass Spring Damper system | 6 |
| 2.3 | Solution | 7 |
| 2.4 | Damping | 7 |
| 2.5 | Harmonic response | 10 |
| 2.6 | Values for k, m and c | 10 |
| 2.7 | Transfer Function | 13 |
| 2.8 | Simulation | 14 |
| 2.9 | Noise | 15 |
| 3 | Mechanical Design | 16 |
| 3.1 | Basic Design | 16 |
| 3.2 | Springs | 17 |
| 3.3 | Damper | 18 |
| 3.4 | Exact design and design conclusion | 18 |
| 3.5 | Electrical Design | 20 |
| 3.6 | Bill of Materials | 20 |
| 4 | Read-out Principles | 22 |
| 4.1 | Capacitive read-out principle | 22 |
| 5 | Building of the accelerometer | 24 |
| 5.1 | Approach for the building process | 24 |
| 5.2 | Leaf springs | 24 |
| 5.3 | Area of the damper | 25 |
| 5.4 | Further building | 26 |
| 6 | Design choice | 27 |
| 7 | Experiment | 28 |
| 7.1 | Experiment 1 | 28 |
| 7.2 | Experiment 2 | 28 |
| 7.3 | Experiment 3 | 28 |
| 8 | Results | 29 |
| 8.1 | Comparison | 31 |
| 9 | Discussion | 32 |
| 9.1 | Observation from results | 32 |
| 10 | Conclusion | 34 |
| 11 | Appendix A | 35 |
| 11.1 | Calculations for equation 2.2 | 35 |
| 11.2 | Derivations for equation 2.5 | 35 |

| | |
|--|-----------|
| 12 Appendix B | 36 |
| 12.1 Piezoresistive read-out principle | 36 |
| 12.2 Piezoelectric read-out principle | 36 |
| 12.3 Resonant frequency read-out principle | 36 |
| 12.4 Inductive read-out principle | 37 |
| 12.5 Optical read-out principle | 37 |
| 12.6 Thermal read-out principle | 37 |
| 12.7 Electron tunneling read-out principle | 38 |
| 13 Appendix C | 39 |
| 14 Appendix D | 40 |
| 15 Appendix E | 43 |

Abstract

This project focuses on the behavior of a self build accelerometer. The application of the accelerometer will be a back-up GPS in case the your satellite GPS fails (e.g. in a tunnel) so the driver does not get lost. To design such a device, the accelerometers' mechanical and electrical design are both of high importance. The first section therefore describes the theory, including the specifications and the derivations for the k , m and c values, as well as simulations. In the second section a mechanical designs plus its possible read out technique will be considered. The mechanical design will consist of a mass connected to two coupled capacitor plates, a water damper and leaf springs. Therefore also a capacitive read out technique was chosen. The last section shows the experiments done on the accelerometer plus how these results were interpreted to come to a conclusion of how it works

1 Introduction

The goal of this project is to design an accelerometer. The whole process from the approach on how to build a working accelerometer to actually building and testing the system is therefore described in this paper.

For the application, it was decided to design an accelerometer that can function as a back-up GPS in case your normal satellite GPS stops working. It should be able to track one's place, but it needs a reference point of where you will start. From that reference point it will detect your acceleration in at least the x and y direction to determine where one is headed. The first part will describe all the theory behind the accelerometer. Here different specifications for the accelerometer will be stated and these need to be followed in order to create the best design. Also the derivation of the k, m and c values of the spring, mass and damper will be explained. In the end a simulation with the given k, m and c values shows that these k, m and c values should work well for the desired accelerometer.

The second part will describe the choice of the mechanical design plus read-out technique. Therefore several mechanical designs and read out techniques were considered and the best combinations were chosen. The mechanical design will, next to a damper, spring and mass, contain a capacitor. Due to the acceleration, there will be a difference in capacitance, which will be measured using the capacitive read-out principle to eventually get the acceleration of the car in a certain direction.

The last part of the paper describes how the right k, m and c values were found for the system to choose the right mechanical design with exact dimensions. This will be shown using a technical drawing. In addition to this the report will show an electrical design for the capacitive read-out principle.

The last part of the paper is the most exciting one. Here the experiments plus its results are stated in several graphs and numbers. These graphs and numbers were of course compared to earlier expected numbers and graphs that were computed in the first phase of the project to get to a final conclusion on how well the accelerometer works and if it is feasible to use it (together with more accelerometers) as a GPS.

2 Theory

2.1 Specifications

| # | Specifications of the accelerometer | |
|----|-------------------------------------|-------------------------|
| 1 | Type of accelerometer | Capacitive |
| 2 | Amplitude range | +/- 4g |
| 3 | Displacement | +/- 2.4cm |
| 4 | Resolution | 0.05g |
| 5 | Shock Limit | 100g |
| 6 | Weight | 1.357kg |
| 7 | Volume | 30 (l) x 30(b) x 10 (h) |
| 8 | Frequency range | 0.0001Hz - 5Hz |
| 9 | Excitation voltage | 10-20V DC |
| 10 | Axis | 1-Axis |
| 11 | Budget | 50,- € |

This project's accelerometer is of capacitive nature using a microcontroller to produce output data. The maximum displacement which the exact design permits is 2.4cm and generates an amplitude range of +/- 4g with a resolution of 0.05g. The system has operated at room temperature throughout testing with a weight of 1.357 KG. During such testing a frequency range of up to 5Hz was found. The resonance frequency of the system lies slightly higher than this at 11Hz. The system was constructed in three different ways regarding its damping: air damped, simple water damped and fully water damped. The design does not permit the system to be used in any other than the horizontal axis. All dimensions of the system can be found in Appendix D and all theoretical calculations regarding further specifications can be found in section 3.6 and 3.7.

2.2 Mass Spring Damper system

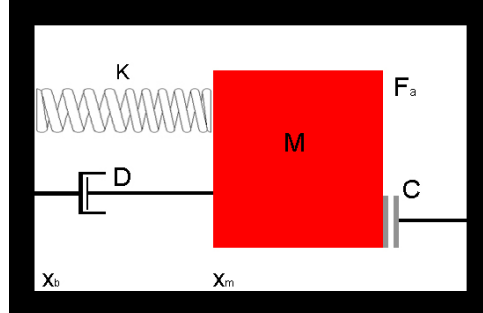


Figure 2.1: The basic model of a mass-spring-damper accelerometer. The mass will vibrate when an acceleration occurs. Therefore the capacitance of the capacitor will change.

As indicated above the accelerometer is in a box. It consists of a spring, a damper and a mass. To measure the acceleration, a capacitor is added. Beginning with the calculations for the accelerometer system and then continuing with the calculations for the capacitors, a final design will be made by simulating the system using simulation software (Simulink®). Since all forces applying on it should be equal to zero in equilibrium as is given in Equation 2.1

$$\sum F = 0 \quad (2.1)$$

The accelerometer consist of different forces. We first specify the direction.

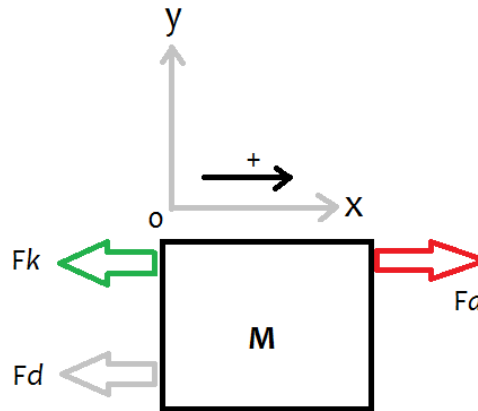


Figure 2.2: Free body Diagram of the mass within the accelerometer

The force of the spring becomes:

$$F_s = -k(x_m - x_b) \quad (2.2)$$

The minus comes from the force of the spring being in the opposite direction of the direction of the mass.

The force of the damper becomes [1] (the deriviatons after this can be seen in the appendix, section 11):

$$F_d = -cv = -c \frac{d(x_m - x_b)}{dt} \quad (2.3)$$

From here the natural frequency of this accelerometer can be defined, $\omega_0 = \sqrt{\frac{k}{m}}$ in rad per sec. The damping factor is defined as $\zeta = \frac{\text{actual damping value}}{\text{critical damping value}} = \frac{c}{2\sqrt{km}} = \frac{c}{2m\omega_0}$ [2].

Now the first equation can be rewritten substituting ζ and ω_0

$$-a = \frac{d^2x}{dt^2} + 2\omega_0\zeta \frac{dx}{dt} + \omega_0^2x \quad (2.4)$$

2.3 Solution

The homogeneous equation becomes:

$$\frac{d^2x}{dt^2} + 2\omega_0\zeta \frac{dx}{dt} + \omega_0^2x = 0 \quad (2.5)$$

Trying $x(t) = e^{rx}$, the characteristic solution becomes: [3]:

$$r^2 + 2\omega_0\zeta r + \omega_0^2 = 0 \quad (2.6)$$

Then

$$r = \frac{-2\omega_0\zeta \pm \sqrt{4\omega_0^2\zeta^2 - 4\omega_0^2}}{2} \quad (2.7)$$

Then $r_1 = \omega_0\zeta + \omega_0\sqrt{\zeta - 1}$ and $r_2 = \omega_0\zeta - \omega_0\sqrt{\zeta - 1}$

The homogeneous solution is then:

$$x(t) = C_1e^{r_1t} + C_2e^{r_2t} \quad (2.8)$$

2.4 Damping

There are three different cases possible for this mass-spring system [3] [4] [5] (in figure 2.3 and figure 2.4 c_1 and c_2 are chosen equal to 1 as a represent graph). Underdamping, overdamping and critical damping can be possible. Because the accelerometer will be critical damped, the graph in figure 2.5 has different values of c_1 and c_2 :

Underdamping $\zeta < 1$

The formula for the underdamped case can be written as a real and imaginary part: $r_{1,2} = -\omega_0\zeta \pm j\omega_0\sqrt{1 - \zeta^2}$. The imaginary part is the damped natural frequency ω_d . $\omega_d = \omega_0\sqrt{1 - \zeta^2}$. As can be seen from the differential equation, when $2\omega_0\zeta = 0$, the response is a sinus wave. Damping is a frictional force and generates heat. If $2\omega_0\zeta$ is small, the system will still oscillate with decreasing amplitude and covert it's energy

to heat. Over a long time it will be rest at equilibrium. In equation 2.14, $e^{-\zeta\omega_0 t}$ represents the decreasing amplitude, the later part represents the oscillation.

The general solution is $x(t) = C_1 e^{r_1 t} + C_2 e^{r_2 t}$. Filling r_1 and r_2 :

$$x(t) = e^{-\zeta\omega_0 t} (C_1 e^{j\omega_d t} + C_2 e^{-j\omega_d t}) \quad (2.9)$$

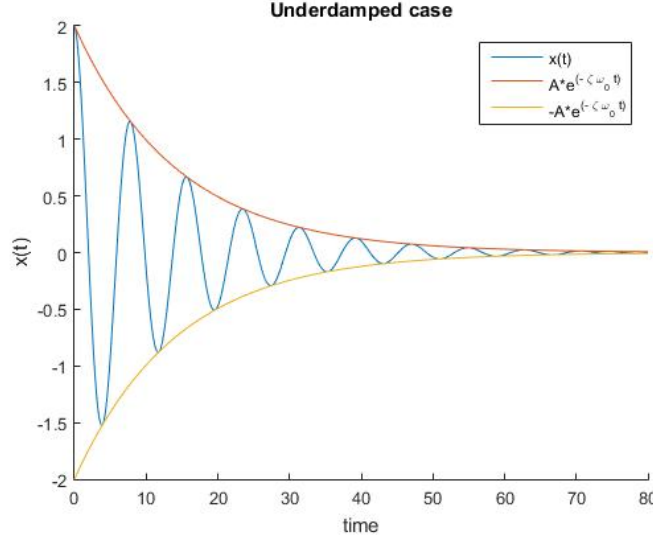


Figure 2.3: An underdamped system where $A = 2, c = 0.7 \text{ Nsm}^{-1}, \omega_0 = 0.1 \text{ Hz}, \omega_d = 0.8 \text{ Hz}, c_1 = 1, c_2 = 1$.

Overdamping $\zeta > 1$

For the the overdamped case, ζ is always greater than 1, thus the root will never be imaginary. That means that the general solution becomes:

$$x(t) = e^{-\zeta\omega_0 t} (C_1 e^{\omega_0 \sqrt{\zeta^2 - 1} t} + C_2 e^{-\omega_0 \sqrt{\zeta^2 - 1} t}) \quad (2.10)$$

From physically, if there is large damping , then frictional force will also be large, so the system will no oscillate any more.

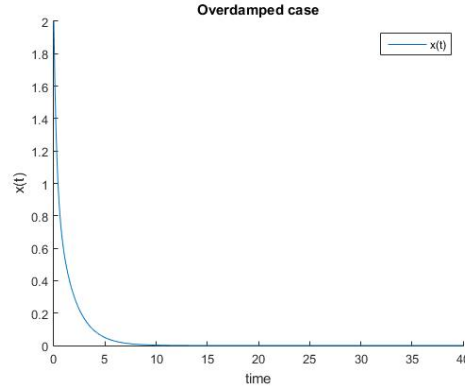


Figure 2.4: An overdamped system where $A = 2, \omega_0 = 1.2, \omega_d = 1.8, c_1 = 1, c_2 = 1$.

Critical damping $\zeta = 1$

For critical damping, $\zeta=1$, so $r_{1,2}$ becomes:

$$r_{1,2} = -\omega_0 \zeta \quad (2.11)$$

That means that the basis of the solutions is

$$C_1 e^{-\zeta \omega_0 t} \quad (2.12)$$

and

$$C_2 t e^{-\zeta \omega_0 t} \quad (2.13)$$

Thus the general solution becomes:

$$x(t) = C_1 e^{-\zeta \omega_0 t} + C_2 t e^{-\zeta \omega_0 t} \quad (2.14)$$

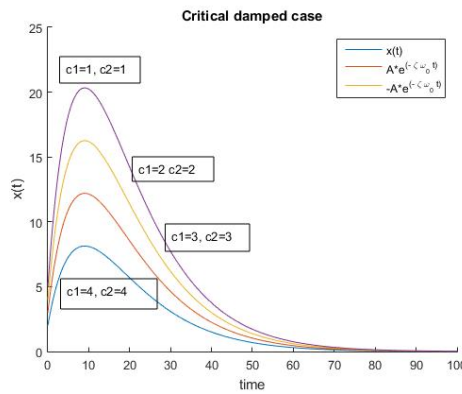


Figure 2.5: A critical damped system for which $\zeta = 1$ and c_1 and c_2 differ from 1 to 4.

The system would be critically damped, such that the system goes back to its 'rest' position as fast as possible. That means $\zeta = 1$.

$$\zeta = \frac{c}{2\sqrt{km}} = 1 \quad (2.15)$$

2.5 Harmonic response

The input signal is actually an acceleration. Thus the force is actually not 0, but the solution is $solution_{homogenous} + solution_{particular}$.

$$\frac{d^2x}{dt^2} + 2\omega_0\zeta\frac{dx}{dt} + \omega_0^2x = asin(\omega_ft) \quad (2.16)$$

The acceleration is described using a sine wave because the acceleration can be described as an oscillation instead of $-a$. The homogeneous solutions as can be seen in equations 2.9, 2.10 and 2.14.

The output signal will be:

$$x_p = C_1cos(\omega_ft) + C_2sin(\omega_ft) \quad (2.17)$$

Where ω_f in the input frequency. The magnitude then becomes (the derivations can be seen in appendix, section section 11).

$$A = \sqrt{C_1^2 + C_2^2} \quad (2.18)$$

And the phase shift becomes

$$\phi = \arctan\left(\frac{C_1}{C_2}\right) \quad (2.19)$$

Then the general solution for critical damping ($\zeta = 1$) becomes

$$x(t) = C_1e^{-\omega_0t} + C_2te^{-\omega_0t} + Asin(\omega_ft + \phi) \quad (2.20)$$

2.6 Values for k, m and c

The value of k, m and c depend on the following formulas

$$\zeta = \frac{c}{2\sqrt{km}} = 1 \quad (2.21)$$

$$\omega_0 = \sqrt{\frac{k}{m}} \quad (2.22)$$

$\zeta = 1$ to have the system critically damped. One would like to operate the accelerometer in the 'flat' region [2] of its frequency range. Thus not close to the natural frequency.

A maximum g force of $4g$ ($a_{max} \approx 39.24m/s^2$) should be measured, but the device should also be shockproof to $\approx 1000g$. From that we can find ω_0 , the natural frequency when the system oscillates. With

$$F = ma = kx, \quad \frac{k}{m} = \frac{a_{max}}{x_{max}} \quad (2.23)$$

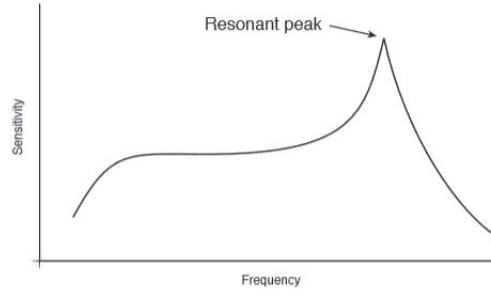


Figure 2.6: Frequency range of an accelerometer [6]

where x_{max} is the maximum distance the body will move under an acceleration of a_{max} . To fit in the dimensions of the intended accelerator a maximum distance of x_{max} of a 2 centimeters was chosen. Together with Equation 2.22 it yields

$$\omega_0 = \sqrt{\frac{a_{max}}{x_{max}}} \quad (2.24)$$

From the specifications a bandwidth of 0.001 Hz to 5 Hz occurs. To be able to measure correctly without a fast increasing amplitude, the natural frequency should be above the 10 Hz. Since ω_0 has the dimensions of $\frac{rad}{s}$ the natural frequency in Hz can be calculated by

$$f_0 = \frac{1}{2\pi}\omega_0 \quad (2.25)$$

Using Eq. 2.22, solving for the spring constant k yields

$$k = \omega_0^2 m \quad (2.26)$$

and together with Eq. 2.21 the damping constant c can be calculated by

$$c = 2\zeta\sqrt{km} = 2\zeta\omega_0 m \quad (2.27)$$

Since the system should be critically damped $\zeta = 1$ Eq. 2.27 simplifies to

$$c = 2\sqrt{km} = 2\omega_0 m \quad (2.28)$$

Now it can be seen that all values heavily depend on the chosen mass.

To find the values for k , m and c , two variables have to be fixed. Maximum acceleration, maximum deviation, mass, spring constant or the natural frequency.

To find suiting values for m , k and c the deviation of the natural frequency is fixed as well as the mass. Furthermore it was convenient to assign the spring constant, damping constant and the maximum acceleration to be neither too low nor too high.

In Table 2.1, 2.2, 2.3 some possible setups are listed.

| $f_0 = 10Hz$ (ms^{-2}) | $\omega_0 = 62.83 \frac{rad}{s}$ | $x_{max} = 0.02m$ | $a_{max} = 8.00g$ |
|-------------------------------|--------------------------------------|------------------------------------|-------------------|
| Mass (kg) | Damping constant c (Nsm^{-1}) | Spring constant k (Nm^{-1}) | |
| 0.1 | 12.57 | 394.78 | |
| 0.2 | 25.13 | 789.57 | |
| 0.3 | 37.70 | 1.18×10^3 | |

Table 2.1: Low natural frequency

| $f_0 = 12Hz$ | $\omega_0 = 75 \frac{rad}{s}$ | $x_{max} = 0.02m$ | $a_{max} = 11.60g$ |
|------------------|--------------------------------------|------------------------------------|--------------------|
| Mass (kg) | Damping constant c (Nsm^{-1}) | Spring constant k (Nm^{-1}) | |
| 0.1 | 15.08 | 568.49 | |
| 0.2 | 30.16 | 1.14×10^3 | |
| 0.3 | 45.24 | 1.71×10^3 | |

Table 2.2: Medium natural frequency - These values will be used.

| $f_0 = 14Hz$ | $\omega_0 = 94 \frac{rad}{s}$ | $x_{max} = 0.02m$ | $a_{max} = 15.78g$ |
|------------------|--------------------------------------|------------------------------------|--------------------|
| Mass (kg) | Damping constant c (Nsm^{-1}) | Spring constant k (Nm^{-1}) | |
| 0.1 | 17.59 | 773.78 | |
| 0.2 | 35.19 | 1.55×10^3 | |
| 0.3 | 52.78 | 2.32×10^3 | |

Table 2.3: High natural frequency

2.7 Transfer Function

Displayed in figure 3.2, one can see that there are 4 forces working in the same direction, namely: F_k (spring force), F_d (damper force), F_a (sum of all forces) and F_s (external force). Where:

$$F_d = cv = cx' \quad (2.29)$$

$$F_k = kx \quad (2.30)$$

$$F_a = ma = mx'' \quad (2.31)$$

These equations together will give the following equation:

$$mx'' = F_s - cx' - kx \quad (2.32)$$

Which is a second order differential equation.

If Laplace is then applied for this equation the following equation is obtained:

$$F(s) = kx(s) + csx(s) - x_0 + ms^2x(s) - x'_0 - sx_0 \quad (2.33)$$

where x_0 and x'_0 are initial conditions.

If it is solved for $x(s)$ this will be the following equation:

$$x(s) = \frac{1}{ms^2 + cs + k} F(s) + x'_0 + (1 + s)x_0 \quad (2.34)$$

Where the first until $F(s)$ is the particular solution or the force response and the rest, the part containing all the initial conditions, is the homogeneous solution or the free response. To find the transfer function, only the particular solution will be needed, which will then give:

$$\frac{x(s)}{F(s)} = \frac{1}{ms^2 + cs + k} \quad (2.35)$$

Which is the transfer function. The preferred system would be in the middle of tables listed above. The transfer function for this accelerometer, using the values in table 2.4, becomes:

$$\frac{x(s)}{F(s)} = \frac{1}{0.2s^2 + 30.16s + 1.13 \times 10^3}$$

| | |
|------------|-------------------------------|
| Mass | 0.2 kg |
| ω_0 | 75.40 rad s^{-1} |
| f_0 | 12Hz |
| c | 30.16 Nsm $^{-1}$ |
| k | 1.13×10^3 Nm $^{-1}$ |
| x_{max} | 0.02 meter |
| a_{max} | 11.6 g |

Table 2.4: K, m and c values for the accelerometer.

2.8 Simulation

For the simulation the following circuit was designed.

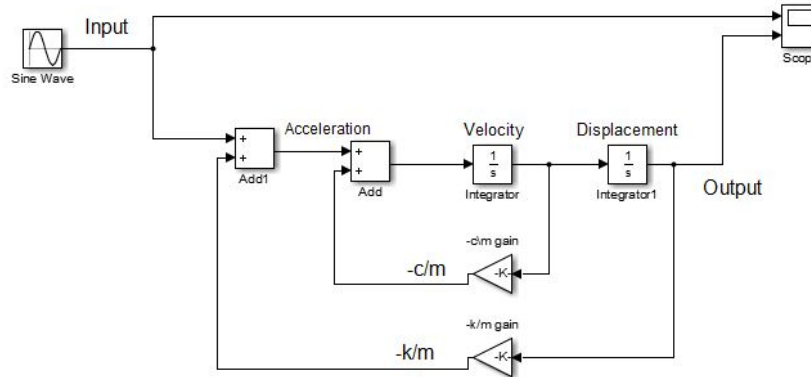


Figure 2.7: Simulink circuit

For the given values of k , m and c in table 2.4, the bode plot becomes:

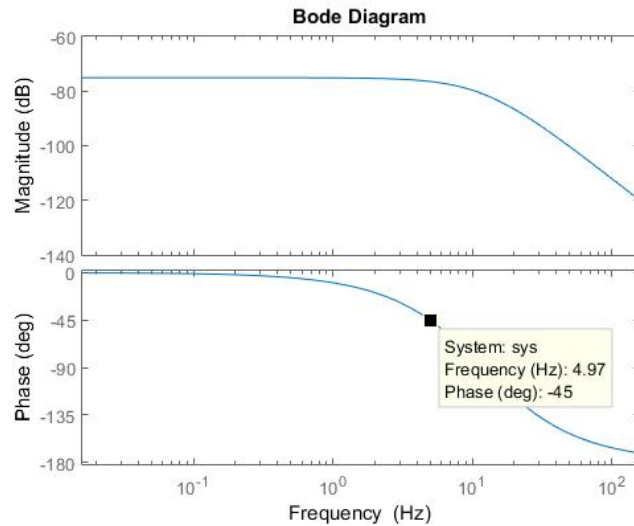


Figure 2.8: Bode diagram for the given values seen in section 2.6

As is seen in this plot, the -3db point is at 4.97Hz. This is quite low, but at -3db, there is still a signal, although decreased. Expectations are that above 5 Hz will not be as important as the lower frequencies.

2.9 Noise

In the accelerometers, Brown noise will affect the accuracy. So it is necessary to calculate the Brown noise of the mass spring system.

The Brown noise force [7]:

$$Fn = \sqrt{4K_B \times T \times c} \quad (2.36)$$

Where K_B is Boltzman constant ($1.38 \times 10^{-23} J/K$), T is absolute temperature and c is the damping coefficient.

To decrease the noise, the quality factor Q or mass m can be increased, or the resonance frequency ω_0 can be minimized.

To calculate the a value using the specifications in section 2.6, $m = 0.2kg$, $\omega_0 = 75.40 \frac{rad}{s}$, $f_0 = 12Hz$, $c = 30.16 \frac{Ns}{m}$ and $T = 290 K$, the noise is at a unit of $10^{-9} g$. It is way too small compared to the measurement one should get, thus the mechanical noise of the system will not affect the overall result.

3 Mechanical Design

3.1 Basic Design

Any two metallic objects in space can have charges and therefore a voltage applied between them. Capacitance is defined as the ratio of charge between those two objects. The simplest capacitor model is two infinitely charged parallel plates, where one plate is charged positive and the other charged negative with a distance d between the two. A schematic model can be seen in Figure 3.1.

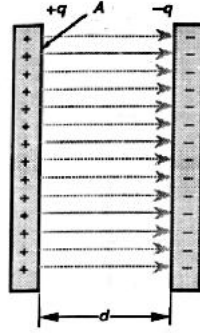


Figure 3.1: Basic model of a capacitor.

The capacitance is then given by

$$C = \frac{\epsilon_0 \epsilon_r A}{d} \quad (3.1)$$

where ϵ_0 is the electric constant ($\epsilon_0 \approx 8.85410^{-12} \text{ Fm}^{-1}$), ϵ_r is the relative static permittivity, a constant dependent on the material between the two plates, the distance d between two plates, and A the area of the two plates.

Therefore the capacitance is linearly dependent on the relative static permittivity ϵ_r , which is a factor depending on the dielectric between the two plates, the area A of the two plates. In this section different mechanical designs will be presented in order to measure acceleration using capacitors.

The most simple idea is to attach one plate to the mass and the other plate to the housing. The mass is attached to the housing by one or more springs and a damper is attached to the mass. Since neither the area nor the relative static permittivity will be changed while having a fixed accelerometer, only the distance d will vary. This fact will be used to measure acceleration and furthermore determine the position of the accelerometer.

One problem is that changing the distance is not linear to the capacitance. The change in capacitance is given by

$$\Delta C = C - C' = \frac{\epsilon_0 \epsilon_r A}{d} - \frac{\epsilon_0 \epsilon_r A}{d'} = \frac{\epsilon_0 \epsilon_r A (d' - d)}{dd'} \quad (3.2)$$

where d' is the distance after movement. A scheme of that system can be seen in Figure 3.2. The restrictions of this design are the incapability to measure in multiple directions. To get information about the acceleration in other directions more of these systems will be needed. To measure in x-, y- and z-axis three of these systems must be aligned in different directions

to work properly. Even with three accelerometers one would still require a gyroscope in order to determine the position of the object.

Another approach is to fix the distance d and to change the the Area A . One plate is fixed at the mass and moves horizontally to the plate fixed at the housing. The basic scheme can be seen in figure 3.2.

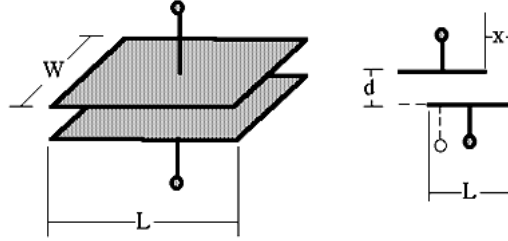


Figure 3.2: Change in capacitance due to horizontal movement.

The measured capacitance would therefore be given by

$$C = \frac{\varepsilon_0 \varepsilon_r L W}{d} = \frac{\varepsilon_0 \varepsilon_r W}{d} (L - x)$$

Since the capacitance is also linearly dependent on ε_r , another approach would be to keep the distance and area fixed and move a dielectric in between the two plates. Having that design in mind the plates would be kept fixed at the housing and a dielectric attached to the mass can move in and out between the plates. This principle is similar to inducing current in a coil with the use of a magnet.

3.2 Springs

As there are different designs for the accelerometer there are different choices which can be made concerning the springs as well. Coil and leaf springs are two possible candidates for the job. Another option would be to use an elastomere (e.g. a rubber band).

Positive side of the coil spring would be that it comes in various sizes and spring constants. Finding or building one is not a big issue. Disadvantage would be that the mass needs to be placed onto a track or transport system to move around. The coil spring on its own is not strong enough to hold up the mass. when the mass is placed on a track or other movement system, the static friction that has to be overcome by the acceleration can be a problem as small accelerations may not be measured by the system.

Leaf springs do not have the problem of not being able to hold the mass up in the air. They are quite strong when used in higher numbers. This way static friction will not be an issue. Although leaf springs can hold up the mass by itself, if one wants to have several centimeters of dielectric between the plates the leaf spring length rises pretty quick. This will result in a wider system, thus will blow up the dimensions of the accelerometer.

Rubber bands or other elastomere have the advantage of being widely available and easy to install. But primary disadvantages will be the non-linear spring constant (the more the

elastomere is elongated the higher the spring constant becomes). Also they can only act in one direction, in other words: these springs are only capable of retracting when pulled upon.

3.3 Damper

Although in calculations it is easier to have a fixed damping coefficient and determine it by varying the mass and spring constant, in a practical application the damping is always present.

Having no damping at all would easily let the accelerometer reach its natural frequency and therefore no acceleration could be measured or the device could be damaged. The damping, as can be seen in Chapter 2.4, should be chosen so that it is critically damped. In a practical way there are different methods to reach the preferred damping. The basic principle is to remove kinetic energy from the moving body, if possible, in a constant matter. Possible ways of application in a self-build accelerometer are using the friction of the body itself on a rail, using a pre-build damper or even immerse the body partially in a liquid with a different viscosity than air. Another way can be to attach some kind of arm on the mass which 'scratches' the housing and therefore adds friction and damping. The friction of the spring itself also has to be concerned. One difficulty will always be the static and kinetic friction. Since when a body is not moving the static friction one needs to overcome to move the body is larger than when the mass is moving already. This can impact the measurements negatively especially in the lower frequencies. When a mass is lifted and not directly connected to the housing the static friction can be decreased to a minimum. Now the static friction is not such a big issue anymore but still there must be some form of damping to slow down the system. The rail-system drops out as it brings the static friction again. Possibilities are now the liquid damping or the 'scratch' damping. Below a small comparison between the two. Liquid damping has some advantages as the liquid is easily interchangeable for another liquid with a higher viscosity for instance. This way the damping constant can be varied quite easily. Negative points would be the possible spills it gives throughout the system and a liquid is also influenced by the acceleration itself which could result in waves occurring in the compartment. This can have a negative reaction on the acceleration of the mass, thus interfering with the measurements. Another problem with the water damping is that the z-axis will be too hard to realize. When looking at the 'scratch' damping advantages would be that it can be easily built and will not give such a mess. Disadvantages are that the mass gets scratched of tiny bit per acceleration. The dampers will reduce the mass of the mass over time. The scratching is also highly non-linear, small deformations in either the mass or the damper itself will cause non-linear movements.

3.4 Exact design and design conclusion

For the exact design of the accelerometer all the earlier given values and calculations will be combined into one system. Below in figure 3.3 the designs for the x- and y-axis are given. Only one system is drawn. But the same principle holds for the other axis. The z-axis will not be considered anymore, an elaborated explanation will be given later in this section.

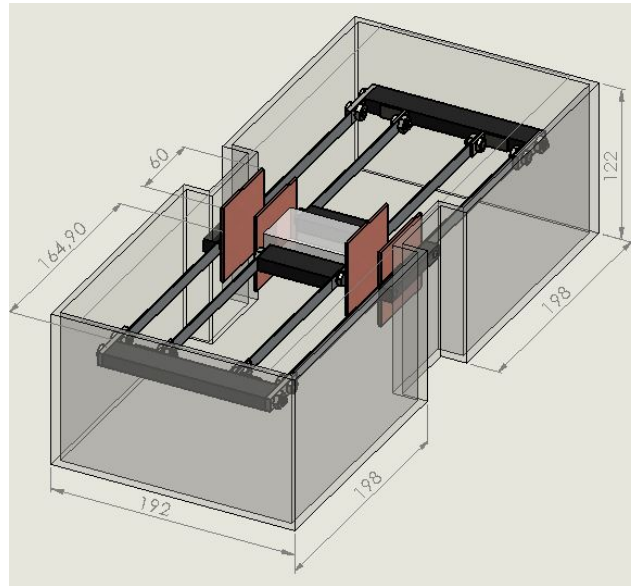


Figure 3.3: Exact design of the accelerometer with $k=1.13 \times 10^3 Nm^{-1}$, $m=0.2 \text{ Kg}$, $c=30.16 \text{ Nsm}^{-1}$.

The total mass which is going to be affected by the acceleration needed to be 200 gram thus the materials could not have a high mass. This resulted in the following design choices. The system in figure 3.3 has a perspex mass in the middle with on either side an aluminum capacitor plate. Perspex has a density of $1.18g/cm^3$ [8] so it will not contribute to much weight to the total mass. Both capacitor plates which are attached on the perspex block are aluminum. This is because it is lighter than copper and only has a minor difference in conductance compared to copper. On either side of the mass one can see two black boxes attached, these were initially PVC and were used as an anchor point for the leaf springs. Later on these were replaced by angle plates as these were lighter. Two leaf springs on each side will go to the outer black rectangles. Again these are PVC and used as attachment points for the springs, but also acts as weight for the total mass. Initial design was to have a threaded end through the PVC block to attach the outer springs but the threaded ends were too heavy so were left out. The holes drilled already in the PVC blocks came in handy as extra weight reduction. The four outer springs connected to the moving PVC are attached to the housing of the accelerometer. Only at these four points the mass makes contact with the housing leaving most of the movable mass freely hanging. Below the mass, not drawn in figure 3.3, is a damper attached. This damper consist of two aluminum plates glued together which will then be surrounded by water. This water is inside a small box on the ground of the housing. An elaboration on calculation of the hanging mass is given in chapter 5.4.

In above's description of the accelerometer design choices have been made. A small elaboration on certain choices is given below. For the springs the leaf spring was chosen as it was strong enough to hold up the mass by itself and thus static friction would not be such an issue. Calculations regarding the leaf springs are given in chapter 5.2 Although harder to build and being a bit messy, as the damper system the one with water was chosen. Primary decision for that was that the system could not be damaged and it really had to be linear

damping. None of these points would be possible with the scratching of the mass. Thus water was chosen to be the damping system.

Now returning to the problem with the z-axis. As water damping is now involved the system will no longer be applicable in the z direction. For the damper to work it then needs to be submerged in water what then also holds for the rest of the accelerometer. With that water then also submerging the capacitor plates and other charged metals, it will probably give false readouts or does not even work. Therefore the z-axis is no longer an option with this particular system.

3.5 Electrical Design

The displacement is proportional to the displacement of the spring in the acceleration sensor. In addition, the capacitance of the capacitive comb in the acceleration sensor can be calculated using

$$C = \frac{\varepsilon_0 \varepsilon_r LW}{d} = \frac{\varepsilon_0 \varepsilon_r LW x}{d^2 - x^2}$$

Therefore, evaluation of carrier vehicle acceleration is done by the displacement x value detection of the proof mass. Where C_1, C_2 are two independent variable capacitors

$$C_1 = \frac{\varepsilon_0 \varepsilon_r LW}{d - x}$$

$$C_2 = \frac{\varepsilon_0 \varepsilon_r LW}{d + x}$$

The capacitive sensing circuit should be connected to a charge amplifier whose output voltage is a function of variations in acceleration. Usually, two configurations are used to measure capacity, that require operational amplifiers as part of their circuits, whose output variables are functions that depend on acceleration variations. Where d the distance between the fixed electrodes and the mobile electrode is a neutral position of the proof mass (zero acceleration), with A common surface area of these electrodes and with the permittivity of dielectric inside the sealed housing of the accelerometer,

3.6 Bill of Materials

In order to spend not too much money on the entire project a bill of materials is made beforehand to get an indication of the expected costs. Below is a table with all the materials and elements. Also with their estimated amounts. Initially the housing of the accelerometer would consist only of perspex. After gathering information it turned out that perspex is quite expensive so only one accelerometer will contain the perspex housing. The other parts will be held together by PVC. The costs in the third column are an estimation and might differ from the actual ones.

| Materials | Weight per piece(gram) | Amount | Cost(€) |
|------------------------------------|------------------------|-----------|----------|
| Perspex mass | 33.04 | 3 piece | 1.50 |
| Capacitor plates (aluminum) | 19.44 | 2 pieces | 1.50 |
| Capacitor plates (copper) | 32.26 | 2 pieces | 3 |
| Leaf springs | 3.54 | 8 pieces | 2.50 |
| 90 degree angled plates (aluminum) | 1.89 | 8 pieces | 1.30 |
| Nuts | 2 | 12 pieces | 0.48 |
| Bolts | 2 | 12 pieces | 0.48 |
| PVC long end | 21.98 | 2 pieces | 0.50 |
| Stiff metal | 4.32 | 4 pieces | 0.80 |
| PVC Box | 1000 | 1 piece | 8 |
| Plate at PVC box | 1.08 | 2 pieces | 0.40 |
| Micro controller | - | 1 piece | borrowed |
| Silicon glue | - | 1 piece | 4.39 |
| Total | - | 1 piece | 24.85 |

4 Read-out Principles

In accelerometer there are two main read-out techniques stress- and displacement-based, both give an output signal corresponding to the acceleration. Piezoresistive, Piezoelectric , and Resonators are all stress based ways of measuring acceleration, whereas displacement based methods are Capacitive, Inductive, Optical, Thermal or Current-tunneling. In this section, the several read-out techniques will be discussed.

4.1 Capacitive read-out principle

In the capacitive read-out principle, one side of the seismic mass, which should be electrically conductive or firmly attached to a movable capacitor plate, forms an electrical capacitance with a counter capacitor plate. Capacitive accelerometers convert the acceleration into a capacitance change. When an acceleration is applied to the accelerometer, the seismic mass deflects from its rest position and changes the capacitance between the mass and the conductive stationary electrodes by a narrow gap. An electronic circuitry can easily measure this capacitance change

In order to have a reasonable capacitance change, the mass and the counter capacitor plate are separated by a few microns ($2\mu m$). This small cavity may lead to an over-damping of the sensor at atmospheric pressure. Thus, the pressure inside the cavity may have to be reduced. Alternatively, holes can be etched through the mass or the counter capacitor plate to decrease the flow resistance of the air.

Capacitive accelerometers have several advantages, which make them very attractive for numerous applications. They have a low temperature dependency unlike piezoresistive accelerometers. Moreover, they have very good DC response, high voltage sensitivity, low noise floor, and low drift. Another important property of the capacitive accelerometers is their low power dissipation, as well as their simple structure

A serious problem with capacitive sensors is that the leads connecting the sensor to the outside show parasitic capacitance which may be of the same order as the sensor capacitance. This makes it very important to place electronic circuitry on or very close to the sensor chip to convert the change in capacitance into an electrical signal. Other disadvantages of the capacitive sensing principle are its high output impedance and the possible presence of leakage resistors. The main advantages of the capacitive read-out principle are low power consumption, high sensitivity, low temperature dependence and high stability.

Most of the research on the accelerometers is based on the capacitive accelerometers, as they provide high sensitivity, low noise floor, and low temperature dependence, making them attractive for the areas where high performance is necessary.

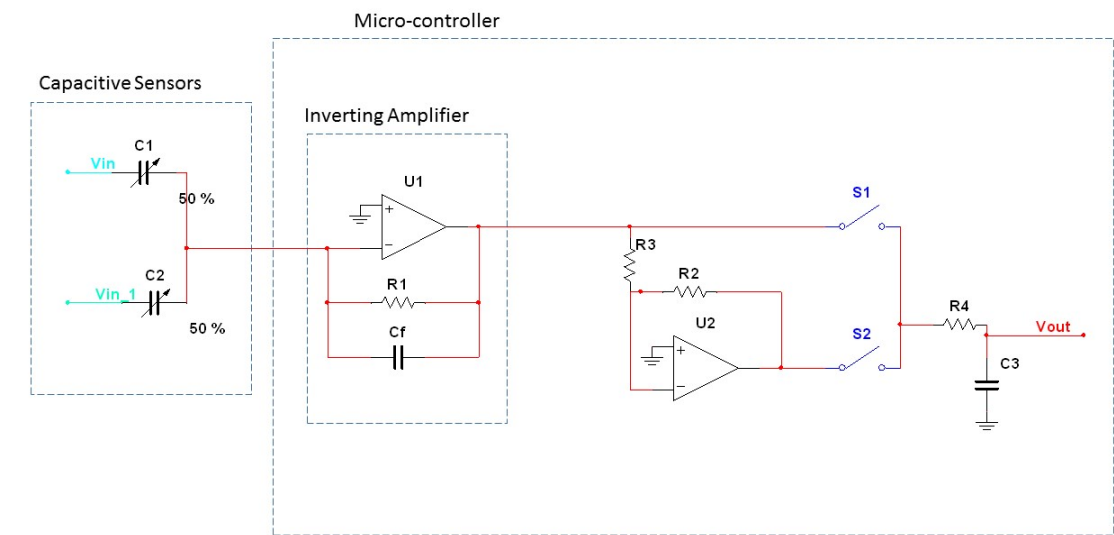


Figure 4.1: Readout Circuit

| | Piezoresistive | Capacitive | Tunneling | Piezoelectric | Optical | Resonant |
|--|----------------|------------|-----------|---------------|---------|----------|
| Sensitivity | | ✓ | ✓ | | ✓ | ✓ |
| Ease of Readout | ✓ | ✓ | | ✓ | | ✓ |
| Independent of Temperature | | ✓ | ✓ | | ✓ | |
| Ease of Construction | ✓ | ✓ | | ✓ | | ✓ |
| DC response | ✓ | ✓ | ✓ | | ✓ | ✓ |
| EMI (electromagnetic interference) Sensitivity | | | | | ✓ | ✓ |
| Noise Floor | | ✓ | ✓ | | ✓ | |

Figure 4.2: Selection Table

5 Building of the accelerometer

5.1 Approach for the building process

Before the building started, several ideas for actual accelerometer types were presented. The technical drawing of the accelerometer can be found in Appendix 14.

5.2 Leaf springs

The relation between the spring constant of a leaf spring and the length of the leaf spring is [9] :

$$K = \frac{E h t^3}{L^3} \quad (5.1)$$

Where E is Young's modulus in Pascal, h is the height in meter, t is the thickness of the spring in meter and L is the beam's length in meter. As can be seen in the appendix 14, the height of the leaf spring is 10 mm and the thickness is 1 mm. According to the model, $k = 1.13 * 10^3 Nm^{-1}$.

The material for leaf springs should be light and Young's modulus should not be too high or too low. If Young's modulus is too high, to keep the same K, L has to be increased then the springs will become very long such that the system itself becomes large. If Young's modulus is low, the springs should be very small. Then it will be hard to obtain the 2 cm difference between plastic and elastic deflection. This lead to aluminum as best available material. For aluminum, Young's modulus equals 69 GPa.

As can be seen in figure 5.1, instead of 1 leaf spring, 8 leaf springs are used. The spring constant is added when they are parallel, $k_1 + k_2 = k_t$. For springs in series, the spring constant becomes $1/K_t = 1/k_1 + 1/k_2$. The two next to each other springs attached to the mass are parallel (2 spring constants). The two outer springs are in series with the two inner springs. That means that the four springs up and down are equal to one spring constant. These parts are in parallel, thus the total spring constant of this system is equal to two spring constants compared to a system with only one spring. Therefore every spring in this system should equal $k/2 = 1.13 * 10^3 / 2$. Using this data, the formula can be rearranged to obtain L.

$$L = \sqrt[3]{\frac{E h t^3}{K/2}} = 0.1069m \quad (5.2)$$

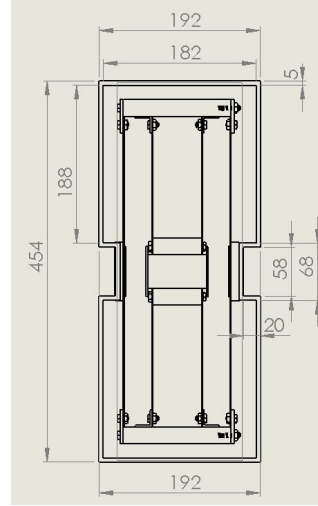


Figure 5.1: Top view of the accelerometer

This is the length the leaf spring should have. Some centimeters are added to be able to clamp the spring. Before starting to build all eight springs, one spring was made and used to calculate the spring constant simply by holding the spring by a clamp with mass attached. At the end of the spring 1 kg (9.81N) was added. The spring constant can then be calculated by $F = -kx$. The spring constant came very close to $k/2$, that the calculated length of 10.69 cm will be used.

5.3 Area of the damper

The damper constant ($c=30.16 \text{ Nsm}^{-1}$) is found using equation 2.16 in page 11. The damping considered for this system is a plate that is damped through a box filled with water. The water will damp the vibration of the mass. To build the accelerometer such that it will be critically damped, Simulink is used to find the area of the damper.

The damping in water is considered as drag [10].

$$F_{drag} = \frac{1}{2} \rho C A v^2 \quad (5.3)$$

ρ is the density, C is the drag coefficient, A the area where the drag is acting on and v is the velocity of the object.

It was assumed that the damper used has a linear dependence of $F_{damping} = cv$. Filling this in equation 5.3 and $\alpha = \frac{1}{2} \rho C$, because they are constants, gives:

$$v = \frac{c}{A \alpha} \quad (5.4)$$

This can be placed in Simulink at $\frac{dx}{dt}$, as is seen in figure 5.2.

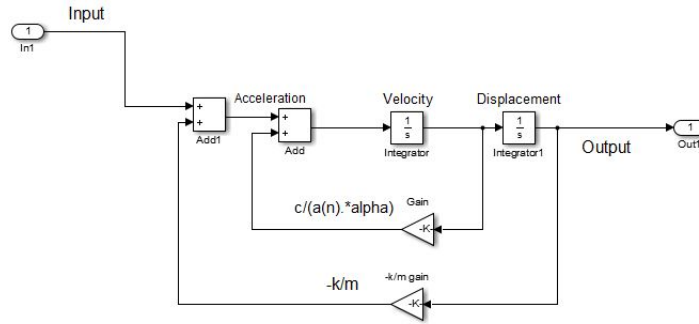


Figure 5.2: Simulink used to find the area of the damper.

As input different values of A are used. After some trial and error, the best value of the area is between 0.0001 m^2 and 0.0019 m^2 as is seen in figure 15.1.

In figure 15.1 the damper should create a critical damped system. This happens when the damper has an area of 10 cm^2 . That will be the case if the fluid used as damper will not create waves.

5.4 Further building

The moving mass of our system included all springs, the PVC long ends, 90 degree angled plates, capacitor plates, bolts, nuts and the perspex mass itself. Seen in Appendix 14. Any glue used was neglected in the mass balance. In table 5.1 the theoretical calculation of all the moving mass is given.

| Part | Quantity | Dimensions(cm^3) | Density(g/cm^3) | Weight(gram) |
|-----------------------------|-----------|----------------------|---------------------|--------------|
| Capacitor plates (aluminum) | 2 pieces | 3.6 | 2.70 | 19.44 |
| PVC long end | 2 pieces | 21.98 | 1.45 | 63.74 |
| Angled plate | 8 pieces | 0.7 | 2.70 | 15.12 |
| Leaf spring (aluminum) | 8 pieces | 1.65 | 2.70 | 35.64 |
| Nut | 12 pieces | - | - | 24 |
| Bolt | 12 pieces | - | - | 24 |
| Perspex mass | 1 piece | 28 | 1.18 | 33.04 |
| Damper | 1 piece | | | |
| Total mass | - | - | - | 214.98 |

Table 5.1: Calculations of total mass

Everything except the perspex mass was built first. Therefore all the parts would be weighed and the mass could be adjusted to this. After all the single parts were made assembling of the inner system could begin. Simultaneously the housing and the damping box could be made. After assembling of the inner part and the housing was done, the two could be combined into the final system. When weighing the inner part the mass turned out to be 230 gram which is a bit more than theoretically calculated. As said before glue weight was neglected and of course dimensions and densities can vary quite a bit from the theoretical part. One thing that has to be considered is that the outer parts of the moving mass, like the PVC and partially the springs, do not contribute as much weight as the perspex mass and capacitor plates would do. Taking this into consideration the mass of the system might actually come pretty close to the desired 200 gram. Exact calculations for which part contributed how much weight was left out as the mass was considered to be close enough to the desired value. This complete system would later on have the electronics attached so that the experimenting could begin. Where the read-out method was done via a micro-controller.

6 Design choice

As a combination of mechanical design and read out technique for the design, the capacitive read out technique plus the accelerometer shown in figure 4.3 were chosen. As the mechanical design contains a capacitor, it is logical to choose the capacitive read out principle. The accelerometer will only measure in one dimension. To use it therefore in real life for the chosen application (GPS without GPS), 3 accelerometers will be needed to measure the acceleration in 3 dimensions. Yet, also a gyroscope may have to be added in order to let it work properly. If the system will move with the car, the different accelerometers will start to measure in different directions leading to a wrong GPS signal. A gyroscope can in the end prevent such mistakes.

The specifications stated in section 2.1 of this paper will be met by choosing the right k , m and c values. The k , m and c values were calculated in section 3.6 and they are: $k = 1130Nm^{-1}$, $m = 0.2kg$ and $c = 30.16Nsm^{-1}$.

7 Experiment

7.1 Experiment 1

Accelerometer test with air damping

Goal: The main objective of this experiment was to find the step response and the frequency response of our accelerometer with air damping. Laboratory Preparation Electronics. A step response is the time evolution of the output of a system to a sudden change in input. By analysing the step response of the accelerometer, the time it needs to come back to its equilibrium state after a sudden application of a force can be investigated. By performing several step response experiments involved simply pulling the proof mass fully to one side and then suddenly releasing it. The voltage output of the system was recorded by a digital oscilloscope and later on evaluated with Matlab. By modelling the response curve, by plotting our output the Quality factor can be obtained of the system together with its natural frequency. The ring down can be seen as an exponential function where the damping coefficient is part of the exponent. As expected from the simulation diagrams, the accelerometer is under-damped. One can see this from the relatively long ring down time, the numerous oscillations with decreasing amplitude which it takes until the proof mass finally comes to rest. A value of $z = 1$ represents a critically damped system. For our system, however it was < 1 . This means that in all three cases of air, half and full water damping our system did not reach critical damping.

Frequency Response:

In this experiment the accelerometer was attached to another device that made it vibrate in one direction at different frequencies (from 5Hz to 14Hz in steps of 0.5Hz, and 20Hz, 40Hz, 80Hz). The voltage that the device gave and the voltage of the reference sensor were measured. These voltages were used to convert it to an acceleration by correcting the RMS voltage to a peak-voltage and multiplying by a constant that depended on the device.

7.2 Experiment 2

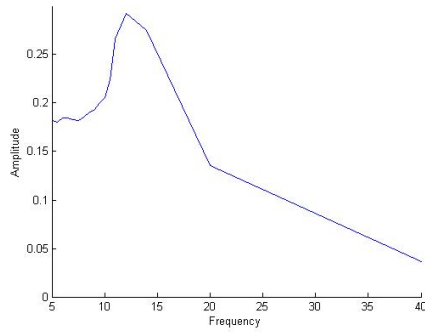
In order to decrease this ringing time and the unwanted oscillations in the step response, the damper box was partially filled with water to add viscous damping on the system. In preparation for different experiments, the box was glued and sealed so that we could fill it with a fluid. Again, same experiments as earlier on were performed. As expected, the ring down time decreased.

7.3 Experiment 3

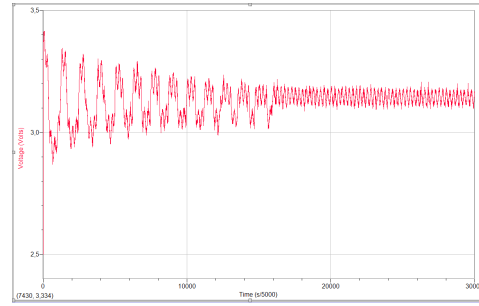
In order to decrease this ringing time and the unwanted oscillations in the step response even more, the damper box was fully filled with water to add more viscous damping. Same experiments were performed as before. As expected, the ring down time decreased even more.

8 Results

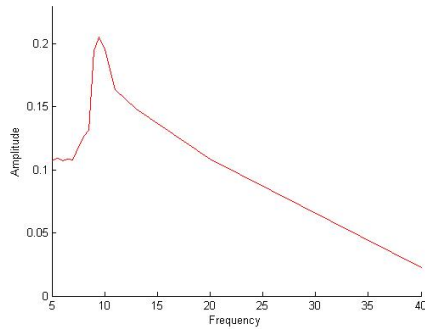
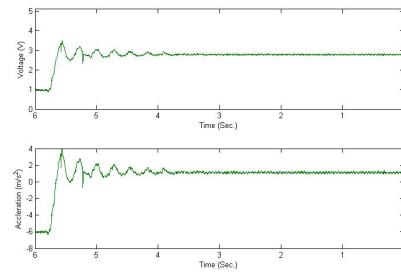
The quality factors for our systems were approximated using the ringdown experiment output data according to the rule that the quality factor may be given by 4.53 times the number of cycles required for the amplitude to half. This produced us with the following values: 18.12, 9.1 and 11.33 for the respective air damping, simple water damping and full water damping systems. The following plots showcase both the output data from the ringdown experiments as well as the bode plots produced from running our system at different frequencies. These bode plots indicate clearly that the resonance frequency of our system is very close to the expected 12Hz. From the slope surrounding the peaks one can make an approximation regarding the magnitude of the quality factors of our systems. This might however be inaccurate due to the low amount of measurements taken surrounding the resonance frequency. The ringdown experiment outputs clearly show the effects of increased damping by the addition of water.

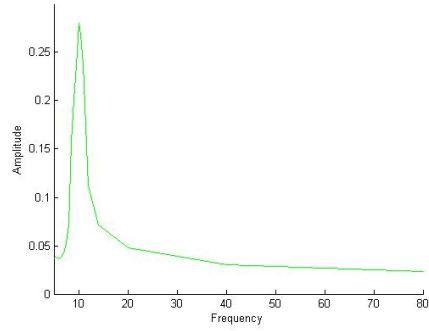


(a) Bode plot with air damping

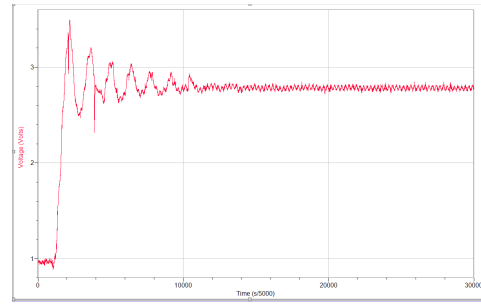


(b) Ring down experiment with air damping

(a) Bode plot with 5 cm² water damping(b) Ring down experiment with 5 cm² water damping



(a) Bode plot with 10 cm^2 damping



(b) Ring down Experiment with 10 cm^2 water damping

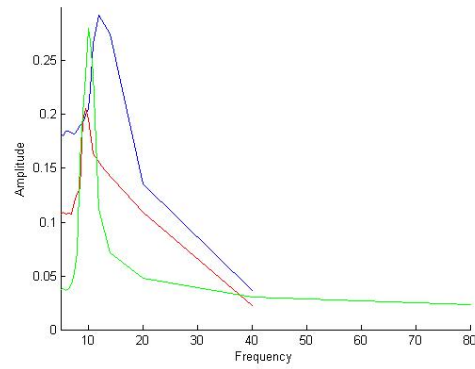


Figure 8.4: Bode plot with air(purple), 5 cm^2 (red) and 10 cm^2 (green) water damping

8.1 Comparison

Comparison with specifications

Figure 8.3a shows that the resonance frequency is around 11 Hz (only full water damped system was considered here) which is right in the middle of the expected resonance frequency of 10-12 Hz. Also figure shows that the frequency range in which it works is about 0 to 4 Hz. From about 4 Hz (again only full water damping was considered here) the system experiences bigger amplitudes, which is not favored for the system. The expected frequency range for this system was 0.001- 5 Hz (see specifications section). This is close to the real frequency range.

Comparison bode plots simulink and experiments

From figure 8.3a, -3db point is about 7 and 12 Hz, resonant frequency is about 11 Hz. While in section 3.8 figure 2.8 the -3db point is at 4.97 Hz. Before doing the experiment, the idea is using a pre-build damper, and the accelerometer is working below 5 Hz. Later it's decided to use water as damper, from figure 8.3a it is easy to see the frequency should be contained below 5 Hz otherwise amplitude will increase dramatically.

Comparison between the different systems

Figure 8.4 shows some clear differences as well. First of all, the resonance frequency of the air damped system (about 14 Hz) is higher than the resonance frequency of the half water and full water damped systems (half water is about 10 Hz, full water is about 11 Hz.) Yet if a resonance frequency should be used to compare with the expected results, the resonance frequency of the fully water damped system should be used as that is the system that will be used in real life.

Next to, the amplitude at resonance of half water damping is smaller than those of full water and air damping. This is something that is not expected, as it is more logical for a system with more damping to have a lower amplitude. So it is expected that full water damping should have a lower resonance amplitude than half water damping which is not the case.

Another critical point for the system is that it is still underdamped. As can be seen in figure 8.3b, the system needs about 7 oscillations to get back to its original position which is far too much. Ideally it should return to equilibrium as quickly as possible without oscillating. Figure 8.1b shows that the air damped system needs about 14 oscillations to return to equilibrium, which is twice as much as for the full water damped system. So the oscillation has halved when a damper area was used of 10cm^2 . In order to fix the damper in the system, the area of the water damper should be doubled from 10cm^2 to 20cm^2 . Then it is expected that the system will be critically damped.

9 Discussion

The most critical factor to improve is of course the damper. As noticed before, the system is quite underdamped. It still needs about 7 oscillations before it goes to equilibrium again, which is far too much. Yet, the new area of the damper can be calculated easily. The number of oscillations to go to equilibrium was halved (from 14 to 7) when a damper with an area of 10cm^2 was added to the system. This means that the area should be doubled in order to get close to the optimal critical damped system that is desired. As the size of the water container is 13 cm by 13 cm by 7 cm, a damper of 10 cm by 2 cm should be perfectly fine for our system. For further experimenting, a larger damper should be added to get better results.

Also, the experimenting did not go flawless. It took a long time before all the wires were soldered or glued onto the accelerometer before the system could be tested properly. This was mostly due to the fact that it is hard to solder a wire onto an aluminum plate. Next to, the equipment that was used was relatively unknown, so it took some time before everyone was accustomed to the equipment. All of this took time to figure out and therefore there was less time to do more measurements for the same experiments. For next time, less time would be needed to get accustomed to the equipment and experimenting will be done a lot faster.

Another point of improvement is of course the accelerometer itself. As it is handmade, it is not perfect. There are tiny flaws in the system that can influence the behavior of the accelerometer in a negative way. The mass was not attached entirely horizontal but a bit skew. Also the mass was somewhat heavier than desired due to unforeseen mass (screws, springs, pvc at the sides), but that didn't seem to be a huge problem during experimenting. It could be that if a smaller total mass was used, the damping would have worked better. There were also problems with the glue, just before the experiments were performed, some of the springs got loose and these had to be glued on right away. These problems are not ones that can be fixed right away the next time as there will always be flaws in the system if the accelerometer is handmade.

Overall there are some things that need to be improved in further testing to ensure the accelerometer would work as desired. The area of the damper should first of all be increased, less time should be spent on figuring out how the testing equipment works so more time can be spent on actual testing and, if possible, fix some tiny flaws in the system itself.

9.1 Observation from results

The accelerometer will only be used when it is fully damped by at least 10 cm^2 . When it is damped like this, the frequency range is from 0 to 4Hz. The desired frequency range is between 0.0001 - 5Hz. The natural frequency is dependent on the spring constant and the mass. To increase the natural frequency, the mass could be made lower or the spring constant higher. Most obvious would be to decrease the mass, therefore the damping would also increase. That is necessary because the system is still underdamped.

In figure 9.5, there is an amplitude at the resonance frequency that is higher than the 5 cm^2 damped or air damped system. The expected issue is that the measurement is done closer to the resonance frequency. Therefore the amplitude is higher, but if the measurements were done on a closer frequency interval, the amplitude of the full water damped system would be the lowest.

Comparing figure 8.1b to figure 8.3b, there is a clear difference in the voltage height in

which the system is oscillating. An explanation for this is that the water in the container is undulating. This will add to the mass that is working on the system, giving the total system a higher mass. Therefore the system behaves different from when no water damping is added. Furthermore this doesn't influence the system, but it is worth noticing. To fix this problem, the water container should have a lid with only a slit for the damper to ensure the water is not able to undulate.

Also the Q-factors of 18.12, 9.1 and 11.33 for the respective air damping, simple watered damping and full water damping systems don't make full sense. As the quality factor is dependent on how well a system is damped, one would expect that the quality factor of the half water system is higher than the full water system as it is less damped. This is not the case however. Yet these numbers were more of an approximation from the ring down experiments. To calculate it more exact, more measurements in the resonance frequency range are needed. So instead of measuring in steps of 0.5 Hz to 1 Hz , steps of 0.2 Hz should be taken. This will result in a sharper and neater peak where more accurate data can be extracted from.

10 Conclusion

Goal of this project was to build a working accelerometer for a certain application. Idea was to build an accelerometer that could determine position of a moving vehicle without the usual GPS satellites. This accelerometer would contain three axis to determine all movements possible. Halfway this project a theoretical action plan was handed in. This needed to contain all the theoretical proof that the proposed system would be feasible to build. After conformation the second part of the project could start where the main goal was to build and test the accelerometer then afterwards compare these results with the theoretical model.

The final design is show in figure 3.3. This final design is quite a bit different than the system proposed in the Mid-Term report. When talking to experts on the subject it became clear that the previous system was not feasible and needed to change. A new system was proposed which was modeled in Solidworks for building. This system contains water damping which resulted in the z direction not being a usable axis anymore. Also it turned out that when one wants to display the position of a moving vehicle, one also needs a gyroscope to keep track of the angles the vehicle makes. This was outside the scope of the project so it was left out of the system. Thus the goal to build a GPS system without satellites was off the table. Now the application was not going to work out but there is still a main goal: building a working accelerometer.

When building, it turned out that the one axis already took up a lot of workshop hours. Thus only one axis was built. With this operational accelerometer the testing began with the results in chapter 8.

From the theoretical model the following values for m, c and k were found: $m = 0.2kg$, $c = 30.16 \frac{Ns}{m}$ and $k = 1.13 \times 10^3 Nm^{-1}$.

From chapter 8.1 several results have been analyzed. The natural frequency from figure 8.3a is around 11 Hz where theoretically 10-12 Hz was expected. Also the working range is from about 0 to 4 Hz where between 0.001 to 5 Hz was expected, the -3db point is about 7 and 12 Hz.

In the end results of the experiment were in accordance with the theoretical model. The system was still underdamped but the methods to solving this problem, add damper area or liquid with another viscosity, are present. Although the liquid turned out to be not entirely linear, see chapter 9, it still acted as a reasonable working system.

Conclusion of this project is that the assignment to build an accelerometer has been met and the system can be improved by the proposed ideas given in chapter 9. The initial goal was not met as one needs one or two more axis and a gyroscope in the system for determining position of a moving vehicle.

11 Appendix A

11.1 Calculations for equation 2.2

The combining equation 2.2 and 2.3 with equation 2.1 as $\frac{d^2 x_m}{dt^2} = \frac{\sum F}{m}$:

$$\frac{d^2 x_m}{dt^2} = \frac{F_s}{m} + \frac{F_d}{m} = -\frac{k}{m}(x_m - x_b) - \frac{c}{m} \frac{d(x_m - x_b)}{dt} \quad (11.1)$$

Thus

$$\frac{d^2 x_m}{dt^2} + k(x_m - x_b) + c \frac{d(x_m - x_b)}{dt} = 0 \quad (11.2)$$

Define $x = x_m - x_b$

$$\frac{d^2 x}{dt^2} + \frac{d^2 x_b}{dt^2} + \frac{c}{m} \frac{dx}{dt} + \frac{k}{m} x = 0 \quad (11.3)$$

Now the force acting on the box is $\frac{d^2 x_b}{dt^2}$, which is an acceleration. Rearrange this with the force function in front.

$$-a = \frac{d^2 x}{dt^2} + \frac{c}{m} \frac{dx}{dt} + \frac{k}{m} x \quad (11.4)$$

11.2 Derivations for equation 2.5

To find the particular solution, the first and second derivative are calculated.

$$x'_p = -C_1 \omega_f \sin(\omega_f t) + C_2 \omega_f \cos(\omega_f t) \quad (11.5)$$

$$x''_p = -C_1 \omega_f^2 \cos(\omega_f t) - C_2 \omega_f^2 \sin(\omega_f t) \quad (11.6)$$

Substituting these equations into equation 2.16

$$[(\omega_0^2 - \omega_f^2)C_1 + 2\zeta\omega_0\omega_f C_2] \cos(\omega_f t) + [-2\zeta\omega_f\omega_0 C_1 + (\omega_0^2 - \omega_f^2)C_2 - F_a] \sin(\omega_f t) = 0 \quad (11.7)$$

Then at $t=0$ the following expression holds

$$(\omega_0^2 - \omega_f^2)C_1 + 2\zeta\omega_0\omega_f C_2 = 0 \quad (11.8)$$

and at $t=\frac{\pi}{2\omega_f}$

$$-2\zeta\omega_f\omega_0 C_1 + (\omega_0^2 - \omega_f^2)C_2 - F_a = 0 \quad (11.9)$$

12 Appendix B

12.1 Piezoresistive read-out principle

A change in specific conductivity is caused due to an applied strain is called piezoresistance. There is a silicon bridge that is calibrated in the zero stress situation, the output voltage due to the imbalance of the bridge is a direct measure of the present stress in the silicon substrate. This stress is proportional, via Hooke's law, to the displacement of the suspended mass and therefore to the applied acceleration. Two advantages of the piezoresistive principle are that a real DC response can be measured (which means it can sense DC accelerations) and no extra electronic circuitry is needed for the detection of the voltage change. There are also major drawbacks of this read-out method. First of all, output voltages of the piezoresistive accelerometers are not very high, typical voltage sensitivities of piezoresistive accelerometers are in the range of $1\text{-}3\text{ mV/g}$. Secondly the strong dependence of the piezoresistive coefficients on temperature causing drifts in sensitivity and high power consumption (a constant current is required to perform continuous measurements). Precise alignment of the piezoresistors with respect to the frame may also cause problems.

12.2 Piezoelectric read-out principle

Acceleration detection of piezoelectric accelerometers is based on applying stress on the piezoelectric material in order to generate charge, proportional to the applied acceleration. A mechanical stress on piezoelectric materials, such as zinc oxide (ZnO), lack inversion symmetry creating internal polarization in response to stress and, reciprocally, an applied electric field generates a mechanical strain.

A major drawback of the piezoelectric read-out principle is the impossibility to measure DC signals since the charge generated on the piezoelectric element leaks away under a constant force, i.e. static accelerations. In addition piezoelectric coefficients of the materials, which determine the sensitivity, are also temperature dependent.

Among the most important advantages of the piezoelectric read-out principle are an excellent behavior at high frequencies, a remarkable stability in time and a negligible power consumption. All these qualities make the piezoelectric accelerometers the best suited to be used as calibrating and reference devices.

12.3 Resonant frequency read-out principle

Resonant accelerometers are force-sensing accelerometers, which directly detect the force applied on the mass. The main difference of the resonant accelerometers from the other types of accelerometers is that they have a continuously resonating mass at its natural frequency under zero acceleration; whereas, the previous accelerometers have stationary seismic masses. Resonant accelerometers senses the change of natural frequency of the vibrating member. When an acceleration is applied, an inertial force acts on the mass of the accelerometer, and this causes a strain in the resonating member of the accelerometer. This strain shifts the resonant frequency of the resonating member according to the sign of the applied stress by the seismic mass. The resonant frequency read-out principle is based on the fact that the resonant frequency of a micro bridge changes when submitted to tensile or compressive stress. By placing these resonant bridges in the beam suspension, the resonant frequency changes with the mass displacement and thus with the acceleration. The resonant frequency can be determined either piezoresistively, capacitively, or optically.

The temperature coefficient of the readout device (piezo-resistors, capacitors or diodes) is not important, because temperature changes merely affect the amplitude of the output signal and not the resonant frequency itself. The remaining thermal behavior of the device is determined by the mechanical and material properties of the sensor, such as Young's modulus and thermally induced stress in the package. Thus, thermal stability remains one of the problems. Other drawbacks are the need for a relatively complex electronic circuitry, including an oscillator, the required presence of an amplifier on silicon accelerometers, the actuator and a sometimes shorter lifetime of the device due to fatigue induced in the permanently oscillating mechanical structure.

12.4 Inductive read-out principle

The electromagnetic acceleration sensor consists of two planar coils, one on the moving mass and one on the containing coil. One of the coils is used to generate an alternating magnetic field. As a result, an induced voltage is generated in the other coil, with an amplitude proportional to the distance between the two coils. In this method the mass displacement and hence the acceleration can be determined.

A disadvantage of this method is that the fabrication of micro-machined coils may cause serious problems.

12.5 Optical read-out principle

Optical read-out principles which have been reported are based on changes in light intensity by the moving mass which acts like a shutter, or by a change in reflected wavelength by using a Bragg grating in a planar waveguide.

The optical read-out principle is very accurate. There are two important advantages of the fiber-optic accelerometers: they are immune to electromagnetic interference, and they have the ability to operate at high temperatures. However, integration of LEDs (Light Emitting Diodes) and detectors with MEMS components for optical generation and sensing is not easy because it requires the implementation of optical devices along with the mechanical sensing structure.

12.6 Thermal read-out principle

In the thermal read-out principle, the operation principle of the first type of accelerometer depends on the principle that the temperature flux from the heat source to the heat sink is inversely proportional with the gap between them. This device uses a seismic mass positioned above a heat source. Due to the heat difference between the heat source and the seismic mass, heat flows from the heat source to the seismic mass. If the gap between the heat source and heat sink is large, there is not much heat flow between the source and the sink, so the heat source remains at the same temperature. The temperature difference is measured using thermopiles.

However, if the seismic mass comes closer to the heat source due to acceleration, a considerable heat flow starts from the source to the sink, which results in a decrease in the temperature of the heat source. The main disadvantage of this method is its high power consumption due to constant dissipation of energy in the heat source.

12.7 Electron tunneling read-out principle

Tunneling accelerometers convert acceleration to a tunneling current. There is always a possibility of electron tunneling between two conductive electrodes, if these electrodes are close enough to each other. The tunneling current is observable when the gap between the two conductive materials is about 10 \AA . As the gap between the conductive materials decreases, the tunneling current increases. Two facts determining the tunneling current between two electrodes are the gap between the electrodes and the sharpness of the tip of the conductive material. As the tip of the conductive material is sharper, the probability of the electron tunneling increases. Because the tunneling only occurs at small values of the gap, the tunneling current is controlled to a constant value in a feedback loop, by controlling either the mass position or the position of the counter capacitor plate, thus ensuring a constant gap. The tunnel current is established between the tip and the seismic mass by a small bias voltage and it depends exponentially on the tip to mass distance. Hence, measuring the tunnel current or the bias voltage necessary to maintain a constant current, the acceleration of the seismic mass can be extracted. Advantage of this method is that it can be used in applications where both a high dynamic range and a high bandwidth are required. Tunneling accelerometers have high sensitivity since tunneling current is highly sensitive to displacement. These devices have small size, wide bandwidth, and high sensitivity, However, they suffer from drift and also $1/f$ noise. In addition, fabrication is not easy. The major drawback of the electron tunneling read-out principle is the need of a high bias voltage of typically 200-300V.

13 Appendix C

Noise calculations

Assuming that in the system, within the frequency range, the displacement of the mass is X , and the response is R . To get the noise response R_n , $X = 0$ and solve R_n in terms of F_n [11].

$$Rn(f) = \sqrt{4K_B * T * C} * \frac{G(f)}{k} \quad (13.1)$$

$$G(f) = \frac{1}{\sqrt{[1 - (\frac{f}{f_0})^2]^2 + \frac{(\frac{f}{f_0})^2}{Q^2}}} \quad (13.2)$$

$$4\pi^2 * f_0^2 = \omega^2 = \frac{k}{m} \quad (13.3)$$

While in the system range f is much smaller than f_0 , the noise Rn becomes:

$$Rn(f) = \frac{\sqrt{4K_B * T * C}}{k} \quad (13.4)$$

We can use a quality factor Q to simplify:

$$Q = \frac{\omega_0 * m}{C} \quad (13.5)$$

$$Rn(f) = \sqrt{\frac{4K_B * T}{\omega_0 k Q}} = \sqrt{\frac{4K_B * T}{\omega_0^3 * m Q}} \quad (13.6)$$

When below the resonance, the response of the mass can be seen as :

$$Rn = \frac{m * a}{k} \quad (13.7)$$

Thus the noise of acceleration is :

$$a = \sqrt{\frac{4K_B * T \omega_0}{m Q}} \quad (13.8)$$

14 Appendix D

Technical 2D drawings of the accelerometer.

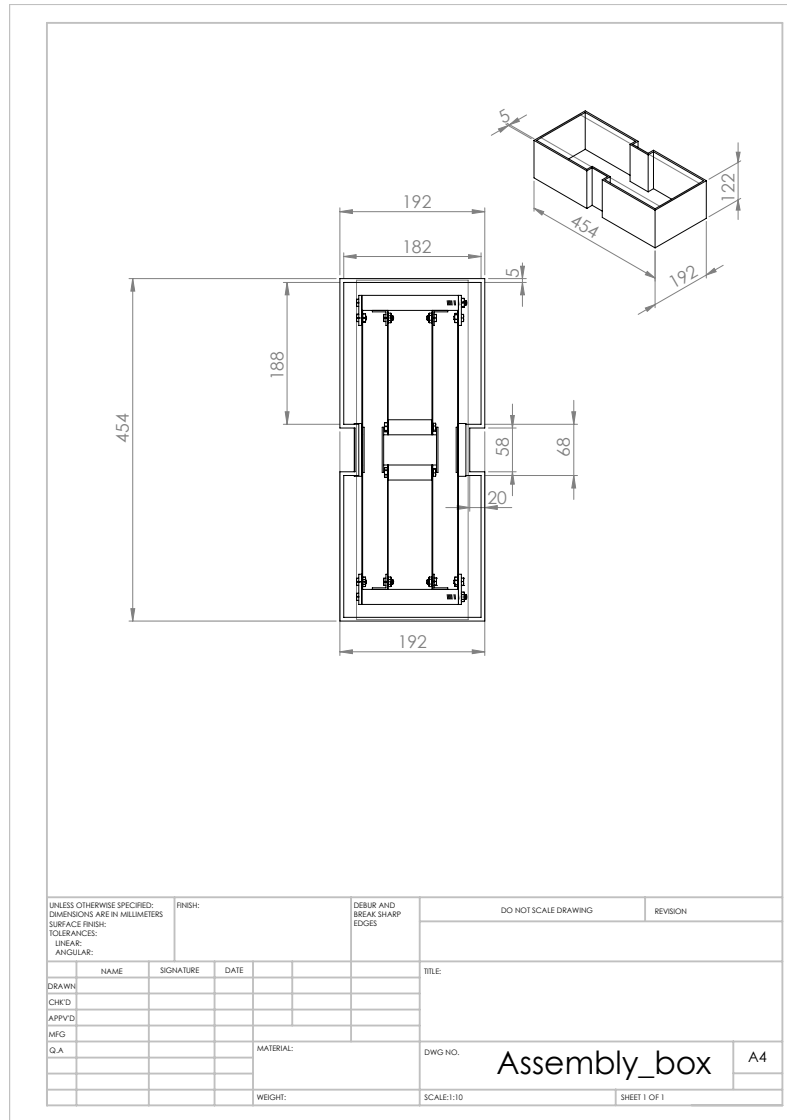


Figure 14.1: dimensions for the box of the accelerometer

15 Appendix E

The page below shows a bode plot for different damping areas. The system should become critical damped. This can be best obtained from the middle bode plot when the area is 10 cm^2 . Then there is no peak anymore and the amplitude before the natural frequency is a straight line as long as possible.

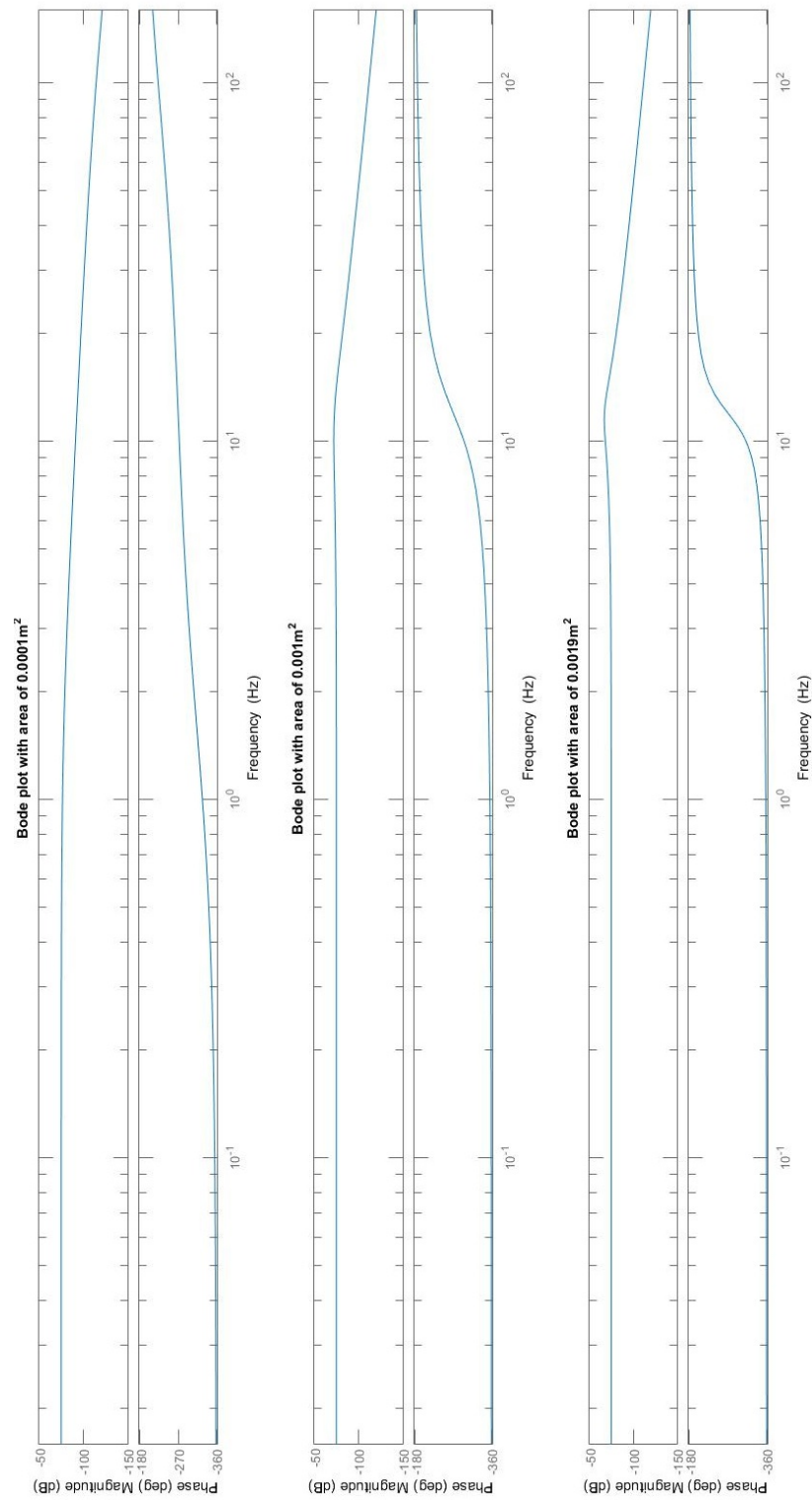


Figure 15.1: Bode plot to find the best area of the damper.

References

- [1] University of California at Berkeley. Accelerometry, February 2005. Visited on 2015.05.14.
- [2] Professor R.G. Longoria. Acceleration measurement and applications, Fall 2011.
- [3] George B. Thomas Jr.; Maurice D. Weir; Joel R. Hass. *Thomas' Calculus: Early Transcendentals*. Number ISBN-13: 978-0321888549. Pearson, 13 edition, October 2013.
- [4] Erwin Kreyszig. *Advanced Engineering Mathematics*. Number ISBN-13: 978-0470646137. Wiley, 10 edition, August 2011.
- [5] Daniel J. Inman. *Engineering Vibration*. Number ISBN-13: 978-0132871693. Prentice Hall, 4 edition, March 2013.
- [6] Practical understanding of key accelerometer specifications, September 2009. Visited on 2015.05.14.
- [7] KAI ZHANG. Sensing and control of mems accelerometers using kalman filter, December 2010. Visited on 2015.05.24.
- [8] Makeitfrom.com. Polymethylmethacrylate (pmma, acrylic), 2015.
- [9] Harmen Droogendijk. Folded leaf springs, 2011. [https : //blackboard.utwente.nl/bbcswebdav/pid - 826998 - dt - content - rid - 15630252/courses/2014 - 201300160 - 2B/folder_leafsprings.pdf](https://blackboard.utwente.nl/bbcswebdav/pid-826998-dt-content-rid-15630252/courses/2014-201300160-2B/folder_leafsprings.pdf), Visited on 2015.06.26.
- [10] Glenn Elert. Aerodynamic drag, 2015. <http://physics.info/drag/>, Visited on 2015.06.15.
- [11] Ville Kaajakari. Mechanical noise in microelectromechanical systems. Visited on 2015.05.24.